We are IntechOpen, the world's leading publisher of Open Access books Built by scientists, for scientists

6,900
Open access books available

185,000
International authors and editors

200M
Downloads

Our authors are among the

154
Countries delivered to

TOP 1%
most cited scientists

12.2%
Contributors from top 500 universities



WEB OF SCIENCE™

Selection of our books indexed in the Book Citation Index in Web of Science™ Core Collection (BKCI)

Interested in publishing with us?
Contact book.department@intechopen.com

Numbers displayed above are based on latest data collected.
For more information visit www.intechopen.com



Chapter

Study of a Novel Liquid-Vapour Separator-Incorporated Gravitational Loop Heat Pipe

Xudong Zhao, Chuangbin Weng, Xingxing Zhang, Zhangyuan Wang and Xinru Wang

Abstract

The aim of this chapter is to report the study of a novel liquid-vapour separator-incorporated gravity-assisted loop heat pipe (GALHP). This involves a dedicated conceptual formation, thermo-fluid analyses, and computer modelling and experimental validation. The innovative feature of the new GALHP is the integration of a dedicated liquid vapour separator on top of the evaporator section, eliminating the potential entrainment between the heat pipe liquid and the steam stream, while addressing the inherent 'dry-out' problem exhibited in the traditional GALHP. Based on this recognised novelty, a dedicated steady-state thermal model covering the mass continuity, energy conservation and Darcy equations were established. Under the specifically defined operational condition, the proposed GALHP has more evenly distributed axial temperature profile. The effective thermal conductivity in the proposed GALHP was 29,968 W/C m. It is therefore concluded that the novel heat pipe could achieve a significantly enhanced heat transport effect. The results derived from this research enabled characterisation of the thermal performance of the proposed GALHP and validation of the developed computer simulation model. The research will enable design, optimisation and analysis of such a new GALHP, thus promoting its wide application and achieving efficient thermal management.

Keywords: LHP, composite wick, start up, thermal conductivity

1. Background

A heat pipe [1, 2] is an effective heat transfer device functioning through the evaporation and condensation cycles without external driving forces, which is normally used under three circumstances: (1) transferring heat from the heat source to heat sink at a distance; (2) transporting a thermal shunt in an effective way and (3) dissipating heat effectively across a plane. To date, various types of heat pipes have been investigated for various applications, for example, electronics cooling, solar devices, heat exchangers, aerospace, medical applications and transportation system [3]. Of these, the most commonly used one is a gravitational straight type, which possesses the problems of increased flow resistances within the vapour and liquid flows and reduced overall heat transport capacity of the heat pipe.

IntechOpen

Loop heat pipe (LHP) [3–5] is a two-phase (liquid/vapour) heat transfer device allowing a high thermal flux to be transported over a distance of up to several tens of metres in a horizontal or vertical position owing to its capillary or gravitational structure. LHP has a separate evaporator and condenser, thus eliminating an entrainment effect occurring in between. LHP can operate under different gravitational regimes, regardless of whether the evaporator is above or below the condenser.

A conventional LHP is usually composed of the complex capillary pumps (evaporators), compensation chambers (storage), condensers and vapour and liquid transfer lines [6–8]. The working principle of the LHP device could be described as follows [1]: the heat transfer fluid in the wick absorbs the heat added to the evaporator and vaporises via the vapour line to the condenser. Within the condenser, the vapour will be condensed to the liquid of the same temperature and return to the compensation chamber through the liquid line. The liquid will then be accumulated and stored in the compensation chamber and further saturate the wick.

Numerous works in relation to LHP have been developed, for example, loop component designs, mathematical models, working fluid and wick structures. The first LHP was developed and tested in 1972 by Russian scientists Gerasimov and Maydanik [9]. A book written by Peterson [10] illustrated the performance limit approach for the heat pipe in the steady-state condition. Peterson [11] also analysed the heat pipe's heat transfer processes in the steady-state condition by using thermal resistances calculating method. In order to simplify the existing engineering models and reduce the required computing resources, Zuo and Faghri [12] developed a thermal network model to analyse the circulation of the working fluid in the heat pipe by using the thermodynamic cycle approach. Kaya and Hoang [13] modelled the performance of a LHP based on steady-state energy balance equations at each component of the loop. The loop operating temperature was found to be a function of the applied power at the given loop condition. Bai et al. [14] established a mathematical model for the start-up process of a LHP based on the node network method. Pauken and Rodriguez [15] modelled and tested a LHP with two different working fluids, that is, ammonia and propylene. Hoang et al. [16] mentioned that the heat transfer characteristic of a LHP was difficult to predict, owing to the complicated nature of the thermal interaction between the LHP and environment. Riehl [17] tested a LHP system operating with acetone as the working fluid. Zan et al. [18] established an experimental formula for a sintered nickel powder wick. Riehl and Dutra [19] presented the development of an experimental LHP. Vlassov and Riehl [20] explored LHP modelling by developing a relatively precise condenser sub-model from the solutions of the conjugate equations of energy, momentum and mass balances, and only describing a few transient nodes within the evaporator and compensation chamber. A more comprehensive dynamic model was published by Launay et al. [21], who proposed a transient model to predict the thermal and hydrodynamic behaviour of a standard LHP.

In recent years, the application of the LHP in solar thermal field has become more and more attractive owing to the significant technical advance in renewable energy [22–24]. LHP is suitable for use in building solar hot water system, owing to its unique features, that is, highly effective thermal conductance and flexible design embodiment and installation [1]. For such an application, the LHP was mostly operated under gravity-assisted conditions, and termed gravitation-assisted loop heat pipe 'GALHP'. The GALHPs have been identified with two shortfalls that need to be tackled with, that is, complicated wick structure and liquid film 'dry-out' problem [3, 4].

In order to overcome the problems exhibited by the conventional GALHP, a novel liquid-vapour separator-incorporated GALHP was proposed, which is dedicated to simplify the wick structure, eliminate the 'dry-out' potential and, thus, create a high-efficient and cost-effective heat transport solution. Through the theoretical and experimental analysis, the analysis results will be compared with the conventional GALHP and conventional straight heat pipe. The research results could be directly used for design, optimisation and analyses of the new GALHP configuration, thus promoting its wide applications in various situations to enable the enhanced performance of the GALHP heat transport to be achieved.

2. Description of the proposed GALHP

Schematic of the proposed GALHP is shown in **Figure 1**, and the novel liquid-vapour separator-incorporated GALHP is shown in **Figure 2**. This separator is configured as a three-way structure, internally containing a tubular pipe with a downward expanding opening, which is fitted into the top of the evaporator while the edge of the expanding opening is tightly attached to the wicked inner surface of the heat pipe. In this way, the return liquid will be reserved in the liquid reservoir above the evaporator, thus formulating a certain liquid head. Under the action of the liquid head, the liquid will penetrate through the peripheral gap between the pipe and the expanding opening, and flow evenly downward along the wicked surface of the heat pipe. Meanwhile, the evaporated fluid, in the form of vapour,

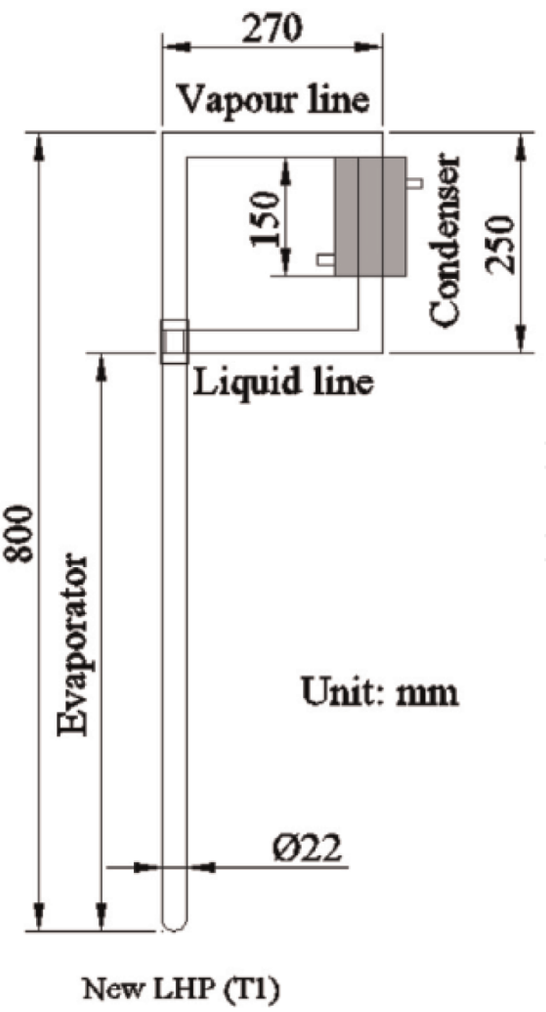


Figure 1.
Schematic of the proposed GALHP.

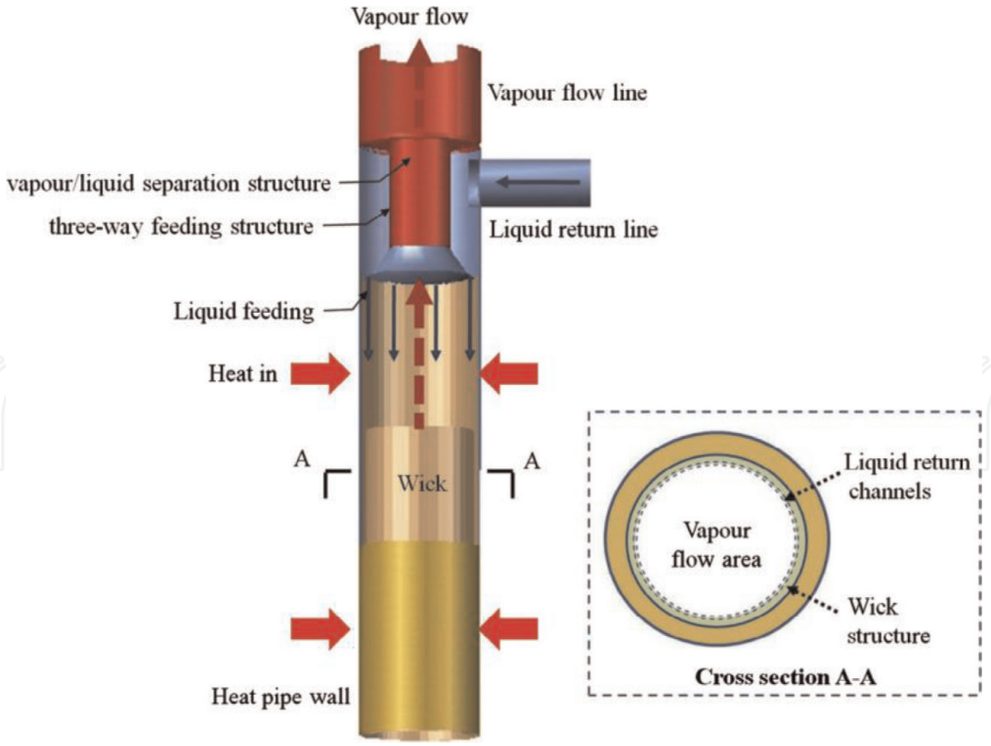


Figure 2.
Top-positioned vapour-liquid separator of new GALHP.

will flow upward through the central tubular pipe and enter into the vapour transport line. If the liquid level is further controlled by a valve mounted on the liquid transfer line, the downward liquid flow rate can be controlled to match the rate of evaporation on the inner surface of the heat pipe. So the wicked inner heat pipe surface will be constantly in 'wet' state, thus preventing the potential 'dry-out' problem with the conventional GALHP. Meanwhile, the vapour and liquid flows will be regulated in the same direction and separated clearly during the operation, thus preventing the potential entrainment problem with the conventional straight heat pipe.

Based on the above innovative concept, a dedicated mathematical model and the associated computer program will be developed to analyse the characteristics of the new GALHP.

3. The model applicable to the proposed GALHP

The mathematical model for the evaporation-condensation processes in the proposed GALHP is based on the following assumptions:

- Heat transfer and fluid flow occur under the quasi-steady-state condition.
- Heat conduction and fluid flow across the wick are one-dimensional in the radial direction.
- Heat pipe evaporator is heated axial-symmetrically and the difference of the temperature along the axial direction is negligible.
- The hydrostatic pressure drop across the radial direction owing to the gravity effect is considered to be zero.

- The axial pressure drop is negligible due to less magnitude against the gravitational head.
- The working fluid is incompressible and has a constant property value in each phase.
- The wick is liquid saturated and wick material is assumed homogenous and isotropic.
- A local thermal equilibrium exists between the porous structure and the working fluid.
- Heat loss to the surroundings is ignored due to the well-insulated pipes.

The mass flow rate within the wick structure is considered to be constant owing to the mass conservation law, given by [4, 16]

$$\dot{m} = \rho_l \mu_l 2\pi\gamma L_{eva} \varepsilon_w = \frac{\dot{Q}}{h_{fg}} \tag{1}$$

3.1 Energy conservation and temperature profile in the evaporator

The energy conservation equations of the single wick structure are given by [4, 25]

$$\frac{\dot{m} C_{pl}}{2\pi r L_{eva}} \frac{\partial T_w}{\partial r} = k_{eff} \frac{1}{r} \frac{\partial}{\partial r} \left(\mathrm{r} \frac{\partial \mathrm{T_w}}{\partial r} \right) \tag{2}$$

The effective thermal conductivity of liquid-saturated wick in a cylindrical geometry is [3, 4]

$$k_{eff} = \frac{k_l[(k_l + k_w) - (1 - \varepsilon_w)(k_l - k_w)]}{[(k_l + k_w) - (1 - \varepsilon_w)(k_l - k_w)]} \tag{3}$$

in which, the porosity of screen wick is expressed as [3, 4]

$$\varepsilon_w = 1 - \frac{1.05\pi n_w D_w}{4} \tag{4}$$

Define the variable α as

$$\alpha = \frac{\dot{m} C_{pl}}{2\pi r L_{eva} k_{eff}} \tag{5}$$

Then, rewrite Eq. (2) as

$$\frac{\partial^2 T_w}{\partial r^2} + \frac{1}{r}(1 - \alpha) \frac{\partial \mathrm{T_w}}{\partial r} = 0 \tag{6}$$

The boundary conditions are

$$\begin{cases} T(r)|_{r=r_{w,0}} = T_{w,0} \\ T(r)|_{r=r_{w,i}} = T_{w,i} \end{cases} \tag{7}$$

By solving the second-order ordinary differential Eq. (6) with twice integrals, temperature distribution in the wick is

$$T(r) = \left[\frac{T_{w,0} - T_{w,i}}{(r_{w,0} - r_{w,i})^{\alpha} - 1}\right] \times \left(\frac{r}{r_{w,i}}\right)^{\alpha} - \frac{T_{w,0} - T_{w,i}(r_{w,0} - r_{w,i})^{\alpha}}{(r_{w,0} - r_{w,i})^{\alpha} - 1} \tag{8}$$

For a single saturated wick layer, the radial thermal conductance is then

$$G_w = \frac{k_{eff} A_{w,i}}{T_{w,0} - T_{w,i}} \times \left.\frac{\partial T_w}{\partial r}\right|_{r=r_{w,i}} = \frac{\dot{m} C_{pl}}{(r_{w,0} - r_{w,i})^{\alpha} - 1} \tag{9}$$

In this case, the temperature distributions are

$$\begin{cases} r_3 \le r \le r_2,\ T(r) = \left[\dfrac{T_{w,2} - T_{w,3}}{(r_2/r_3)^{\alpha_2} - 1}\right] \times \left(\dfrac{r}{r_3}\right)^{\alpha_2} - \dfrac{T_{w,2} - T_{w,3}(r_2/r_3)^{\alpha_2}}{(r_2/r_3)^{\alpha_2} - 1} \\ r_2 \le r \le r_1,\ T(r) = \left[\dfrac{T_{w,1} - T_{w,2}}{(r_1/r_2)^{\alpha_1} - 1}\right] \times \left(\dfrac{r}{r_2}\right)^{\alpha_1} - \dfrac{T_{w,1} - T_{w,2}(r_1/r_2)^{\alpha_1}}{(r_1/r_2)^{\alpha_1} - 1} \\ r_1 \le r \le r_0,\ T(r) = T_{w,1} + \dfrac{(T_{eva,wall} - T_{w,1})}{\ln\left(\dfrac{r_0}{r_1}\right)} \ln\left(\dfrac{r}{r_1}\right) \end{cases} \tag{10}$$

Thermal conductance of the inner and outer wick layers are respectively

$$\begin{cases} G_{w,0} = \dfrac{k_{eff,0} A_{w,2}}{T_{w,1} - T_{w,2}} \times \left.\dfrac{\partial T_w}{\partial r}\right|_{r=r_{w,2}} = \dfrac{\dot{m} C_{pl}}{(r_1/r_2)^{\alpha_1} - 1} \\ G_{w,i} = \dfrac{k_{eff,i} A_{w,3}}{T_{w,2} - T_{w,3}} \times \left.\dfrac{\partial T_w}{\partial r}\right|_{r=r_{w,3}} = \dfrac{\dot{m} C_{pl}}{(r_2/r_3)^{\alpha_2} - 1} \end{cases} \tag{11}$$

and

$$\begin{cases} \alpha_1 = \dfrac{\dot{m} C_{pl}}{2\pi k_{eff,0} L_{eva}} \\ \alpha_2 = \dfrac{\dot{m} C_{pl}}{2\pi k_{eff,i} L_{eva}} \end{cases} \tag{12}$$

$$\begin{cases} k_{eff,0} = \dfrac{k_l[(k_l + k_{w,0}) - (1 - \varepsilon_{w,0})(k_l - k_{w,0})]}{[(k_l + k_{w,0}) - (1 - \varepsilon_{w,0})(k_l - k_{w,0})]} \\ k_{eff,i} = \dfrac{k_l[(k_l + k_{w,i}) - (1 - \varepsilon_{w,i})(k_l - k_{w,i})]}{[(k_l + k_{w,i}) - (1 - \varepsilon_{w,i})(k_l - k_{w,i})]} \end{cases} \tag{13}$$

As a result, the overall thermal conductance of the composite wick structure can be given by

$$G_w = \frac{k_{eff,i} A_{w,3}}{T_{w,1} - T_{w,3}} \times \left.\frac{\partial T_w}{\partial r}\right|_{r=r_{w,3}} = \frac{T_{w,2} - T_{w,3}}{T_{w,1} - T_{w,3}} \times \frac{k_{eff,i} A_{w,3}}{T_{w,2} - T_{w,3}} \times \left.\frac{\partial T_w}{\partial r}\right|_{r=r_{w,3}} = \frac{T_{w,2} - T_{w,3}}{T_{w,1} - T_{w,3}} \times G_{w,i} \tag{14}$$

According to energy conservation, heat flux at the internal surface of the outer wick layer should be equal to the heat flux at the external surface of the inner wick layer

$$k_{eff,0}\left.\frac{\partial T_w}{\partial r}\right|_{r=r_{w,2^+}} = k_{eff,i}\left.\frac{\partial T_w}{\partial r}\right|_{r=r_{w,2^-}} \tag{15}$$

Putting Eq. (10) into the above expression results in

$$\frac{T_{w,1}-T_{w,2}}{(r_1/r_2)^{\alpha_1}-1} = \left[\frac{T_{w,2}-T_{w,3}}{(r_2/r_3)^{\alpha_2}-1}\right] \times \left(\frac{r_2}{r_3}\right)^{\alpha_2} \tag{16}$$

Put Eq. (11) into Eq. (16) and it becomes

$$G_{w,0}(T_{w,1}-T_{w,2}) = G_{w,i}(T_{w,2}-T_{w,3}) + \dot{m}C_{pl}(T_{w,2}-T_{w,3}) \tag{17}$$

Rewrite Eq. (17) as

$$T_{w,2} = \frac{G_{w,0}T_{w,1} + \left(G_{w,i}+\dot{m}C_{pl}\right)T_{w,3}}{G_{w,0}+G_{w,i}+\dot{m}C_{pl}} \tag{18}$$

Put Eq. (18) into Eq. (14) for obtaining the expression of the composite wick structure,

$$G_w = \frac{G_{w,0}G_{w,i}}{G_{w,0}+G_{w,i}+\dot{m}C_{pl}} \tag{19}$$

The thermal resistance in this region is therefore

$$R_{eva} = \frac{\ln\left(\frac{r_0}{r_1}\right)}{2\pi L_{eva}k_{eva,wall}} + \frac{1}{G_w} \tag{20}$$

The interface temperature conditions can be assumed local thermal equilibrium

$$T_{w,3} = T_v = T_{int} \tag{21}$$

3.2 Flow characteristic

In a heat pipe, the maximum capillary pumping head ($\Delta P_{c,\max}$) must be greater than or at least equal to the total pressure drops (ΔP) along the heat pipe. The total pressure drops (ΔP) should be the sum of pressure drops in all the heat pipe components, that is, wick structure, evaporator, three-way separator, vapour line, condenser and liquid line.

$$\Delta P_{c,\max} + \Delta P_g \geq \Delta P \tag{22}$$

$$\Delta P = \Delta P_w + \Delta P_{eva} + \Delta P_{tw} + \Delta P_{vl} + \Delta P_{cond} + \Delta P_{ll} \tag{23}$$

4. Design and fabrication of the proposed GALHP

Based on the results derived from the theoretical and computer simulation studies [26], the proposed GALHP was designed, fabricated and presented in **Figure 3** respectively. For the evaporator, the length remained 550 mm and diameter fixed to 22 mm. Within the inner surfaces of the evaporator, the compound screen mesh wick structure was applied with the size of 160 × 60 mm.

For the condenser, they were all fixed with a steel cooling jacket of the same size, with a length of 150 mm and a diameter of 105 mm. The detailed design parameters are illustrated in **Table 1**.

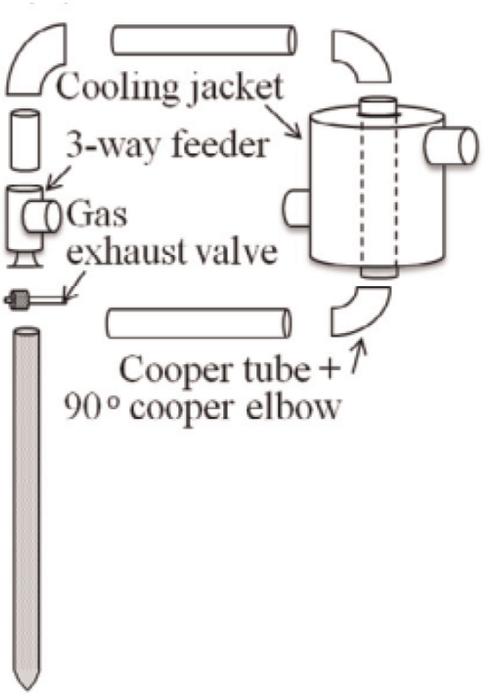


Figure 3.
Fabrication schematics of the proposed GALHP.

Parameters	Nomenclature	Value
External diameter of evaporator (mm)	$D_{hp,o}$	22
Internal diameter of evaporator (mm)	$D_{hp,in}$	19.6
T1: internal diameter of vapour channel in three-way fitting (mm)	$D_{tw,in}$	14
Operating pressure in heat pipe (Pa)	P_{hp}	1.3×10^{-4}
Evaporator length (mm)	$L_{hp,ev}$	550
Liquid filling volume (ml)	V_{fl}	85
Transportation line's outer diameter (mm)	$D_{ll,o}/D_{vl,o}$	22
Transportation line's inner diameter (mm)	$D_{ll,in}/D_{vl,in}$	19.6
Lengths of vapour/liquid /line (mm)	$L_{vl,T1}/L_{ll,T1}$	595/445
	$L_{vl,T2}/L_{ll,T2}$	595/1145
Mesh screen wire diameter (layer I) (mm)	$D_{owi,ms}$	7.175×10^{-2}
Mesh screen layer thickness (layer I) (mm)	$d_{owi,ms}$	3.75×10^{-1}
Mesh number (layer I) (/m)	$N_{owi,ms}$	6299
Mesh screen wire diameter (layer II) (mm)	$D_{iwi,ms}$	12.23×10^{-2}
Mesh screen layer thickness (layer II) (mm)	$d_{iwi,ms}$	3.75×10^{-1}
Mesh number (layer II) (/m)	$N_{iwi,ms}$	2362
Mesh screen conductivity (W/m °C)	k_{ms}	394

Table 1.
Design parameters of the proposed GALHP.

5. Experimental set-up and procedure

5.1 Experimental set-up and instrumentation

Figure 4 shows the test rig of the proposed GALHP. In the rig, an electrical heating tap with the percentage controller, which acts as the heat source, was evenly attached to the external surfaces of the evaporators. The condenser is covered by a steel cooling jacket that allows cooling water to pass through, removing heat from the condenser. A magnetic regeneration water pump was installed in the cooling water loop to power the cooling water cross. A clamp-supported retort stand was used to adjust the inclination angle of the piping installation. The foamy polyurethane was attached to the pipes to provide a satisfactory insulation. During operation, in order to keep a relatively constant condensation temperature, the water tap would remain open to enable adequate amount of cold water to be fed into the loop. When the water tank was fully charged, the drainage valve would be turned open to allow the extra amount of water to be discharged.

A list of the piping elements and test instruments are provided in **Table 2**. A number of T-type thermocouples were attached to the external surface of heat pipe walls, and installed in the inlet/outlet and inside of cooling jacket and water tank: there were totally four thermocouples (No. 1–4) equidistantly attached along each heat pipe evaporator wall from top to bottom, which were used to measure the temperature distribution along the evaporator wall and their corresponding average temperature at the evaporation sections; another four thermocouples were respectively placed in the mid of heat pipe condenser wall (No. 7), the inlet/outlet

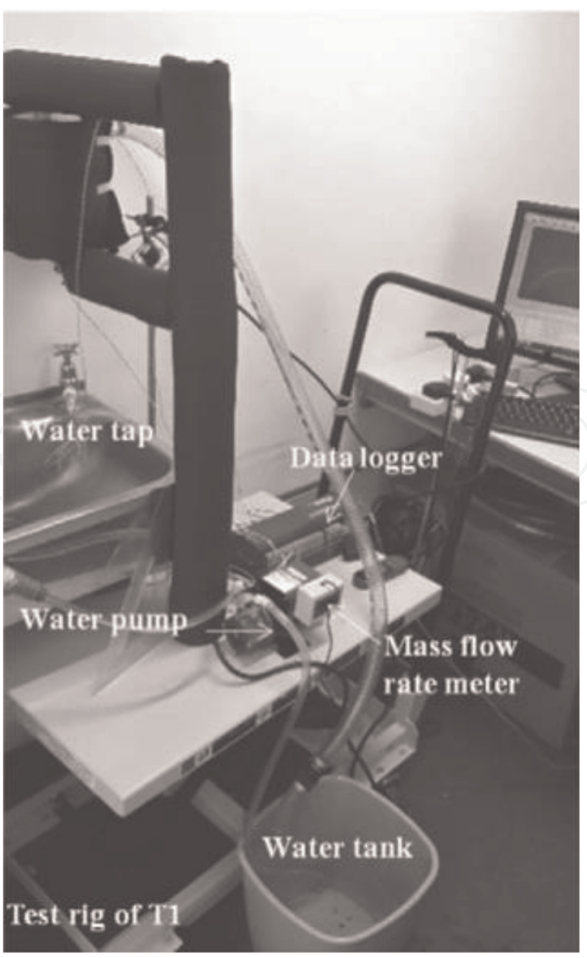


Figure 4.
On-site testing rig.

No.	Name	Model no.	Description
1	PVC-U ball valve	RS: 282-5148	Compression fitting size: 20mm
2	PVC-U hose connector	RS: 212-3638	1/2in BSPT MX20 mm
3	George fischer 90° PVC-U elbow	RS: 279-0575	25 × 25 mm, L. 33 mm
4	Armorvin HNA hose	RS: 339-9921	Clear 5 m × 20 mm ID
5	Magnetically coupled regenerative pump	Totton: HPR6/8	Max capacity: 5.5 l/min Max head: 7.4 m
6	Heating tapes with percentage controller	Omega: HTWC102-004	Length: 1220 mm 14.4–288 w; 240 V; ±0.5 W
7	Black nitrile rubber pipe insulation	RS: 486-053	∅ 22 × 25 mm
			k = 0.035 W/m °C at 0°C
			0.037 W/m °C at 20°C
			0.040 W/m °C at 40°C Min/max temperature sensed
8	T-type thermocouple	RS: 621–2164	Min/max temperature sensed: ±0.1°C, 200–350°C Probe diameter: 0.3 mm
9	1/2" LCD Water fluid flow sensor meter digital display rate turbine flow meter		Flow rate range: 1.5–25.0 l/m, fitting for 1/200, BSP: ±0.1 l/m, water temperature range: 0–80°C
10	Data logger and data recording equipment	TD500 series 3	10 channels DataTaker; ±0.16% 5-s interval recording

Table 2.
List of piping connectors and experimental instruments.

Test mode	Applied heat load (W)	Inclination angle (°)	Cooling-fluid temperature (°C)	Flow rates of cooling fluid (l/min)
Standard	100.8	90	10 ± 0.5	1 ± 0.2
1	14.4	90	10 ± 0.5	1 ± 0.2
	43.2			
	100.8			
	129.6			
2	100.8	90	10 ± 0.5	1 ± 0.2
		60		
		30		
3	100.8	90	10 ± 0.5	1 ± 0.2
			15 ± 0.5	
			20 ± 0.5	
4	100.8	90	10 ± 0.5	1 ± 0.2
				2 ± 0.2
				3 ± 0.2

Table 3.
List of operational modes (parameters) for simulation of the three heat pipes.

Q (W)	u (°)	T_{cf} (°C)	m_{cf} (l/m)	T_{eva} (exp) (°C)	T_{eva} (sim)	CR (−)	E (%)	U (%)	R (exp) (°C/W)	R (sim)	CR (−)	E (%)	U (%)	Start-up (s)
14.4	90	10	1	31.31	34.12	0.8346	6.61	8.05	0.32	0.32	0.9533	18.18	10.63	840
43.2				40.04	36.41			7.34	0.27	0.21			8.26	780
129.6				42.11	43.28			8.00	0.08	0.09			10.26	280
100.8				41.14	40.99			6.80	0.11	0.10			9.46	410
	60			46.72	45.65	0.9825	1.30	5.65	0.13	0.15	0.9995	11.88	6.19	960
	30			48.90	49.43			5.97	0.16	0.20			11.47	1210
	90	15		56.53	48.65	0.8827	8.14	9.98	0.15	0.18	0.9855	13.76	12.36	370
		20		56.92	55.99			7.94	0.14	0.17			9.42	320
		10	2	40.96	38.65	0.9413	6.26	8.89	0.11	0.09	0.9556	13.71	10.65	380
			3	39.95	35.99			10.81	0.10	0.08			11.76	360

Table 4.
Comparison of testing and simulation results of the three heat pipes under different modes.

(No. 5/6) of cooling jacket and the mid of water tank (No. 8) to measure their related average temperature; there were still four more thermal couples applied to measure the temperatures at the vapour (No. 9, 11) and liquid (No. 10, 12) transportation lines; all these thermocouples were further connected to a data logger to record the temperature signals at each testing interval. A control box is provided to adjust the power output of the heating belt, which is considered a thermal load.

5.2 Experimental process

A series of laboratory steady-state tests were carried out and the results of the tests were used to evaluate the thermal performance of the proposed GALHP. The testing conditions are displayed in **Table 3**. During all the sets of tests, the surrounding air temperature and speed were maintained at 20 ± 2°C and 0.01 m/s, respectively. Under initial test conditions, one parameter is changed and the other parameter remains fixed, enabling the development of a correlation between the heat pipe's heat output and associated operating parameters. Once the steady-state conditions have been achieved, the test period is successive 10 h period. The measurement data will be recorded at 5-s interval and logged into the computer system using the DT500 data logger to enable the follow-up analyses to be undertaken.

6. Computer model validation using the experimental results

Table 4 provides the comparison between the testing and the simulation results under all selected testing conditions. The mean correlation coefficient (CR) was found no less than 0.8346 and the root mean square percentage deviation (E) was below 18.18%. This indicated that the developed simulation model could predict the thermal performance at a reasonable accuracy. The differences resolved above may be caused by theoretical and/or inaccurate measurements. From the theoretical side, some simplified assumptions and empirical equations were involved; from the experimental side, a few of the uncertainties addressed above may be the potential reasons for the deviation. Based on these considerations, the errors may be attributed to the theoretical inaccuracies and it would be better for the simulation model to be refined to further improve its accuracy in making predictions based on the experimental results.

7. Conclusion

This chapter reported the study of a novel liquid-vapour separator-incorporated gravity-assisted loop heat pipe (GALHP), which was designed, constructed, and tested. A parallel comparison between simulation and experimental results was made.

Under the specified operational conditions, the start-up timing of the proposed GALHP was 410 s. The overall thermal resistance was 0.11°C/W, indicating that it has small heat transfer resistance owing to its unique structure that led to the even liquid film distribution and thus reduced flow resistance. The actual effective thermal conductivity was 29,968 W/°C m, indicating that it achieved significant improvement in terms of heat transfer. All of these data provide evidence that the proposed GALHP is a super-performance heat transfer device that can be widely used in gravity-assisted heat transfer operations to achieve significant thermal management in a variety of practical applications.

IntechOpen

Author details

Xudong Zhao[1*], Chuangbin Weng[2], Xingxing Zhang[3], Zhangyuan Wang[2] and Xinru Wang[4]

1 School of Engineering, University of Hull, UK

2 School of Civil and Transportation Engineering, Guangdong University of Technology, Guangzhou, China

3 Department of Energy, Forest and Built Environments, Dalarna University, Falun, Sweden

4 Department of Architecture and Built Environment, University of Nottingham, Ningbo, China

*Address all correspondence to: xudong.zhao@hull.ac.uk

IntechOpen

© 2019 The Author(s). Licensee IntechOpen. This chapter is distributed under the terms of the Creative Commons Attribution License (http://creativecommons.org/licenses/by/3.0), which permits unrestricted use, distribution, and reproduction in any medium, provided the original work is properly cited. CC BY

References

[1] Wang Z, Yang W. A review on loop heat pipe for use in solar water heating. Energy and Buildings. 2014;**79**:143-154

[2] Zhang H, Zhuang J. Research, development and industrial application of heat pipe technology in China. Applied Thermal Engineering. 2003;**23**: 1067-1083

[3] Amir F. Heat Pipe Science and Technology. 1st ed. UK: Taylor & Francis Group; 1995

[4] David R, Peter K. Heat Pipes: Theory, Design and Applications. 5th ed. UK: Elsevier; 2006

[5] Maidanik YF. Loop heat pipes. Applied Thermal Engineering. 2005;**25**: 635-657

[6] Dunn PD, Reay DA. The heat pipes. Physics in Technology. 1973;**4**:187-201

[7] Reay D, Kew P. Heat Pipe. 5th ed. London, UK: Elsevier; 2006

[8] Xu X, Wang S, Wang J, Xiao F. Active pipe-embedded structures in buildings for utilizing low-grade energy sources: A review. Energy and Buildings. 2010;**42**:1567-1581

[9] Maidanik YF, Vershinin S, Kholodov V, Dolgirev J. Heat Transfer Apparatus, US patent 4515209; 1985

[10] Peterson GP. An Introduction to Heat Pipes: Modelling, Testing, and Applications. New York: Wiley-Interscience Press; 1994

[11] Ratios of Specific Heat. 2009. Available from: http://www.engineeringtoolbox.com/specific-heat-ratio-d608.html [Accessed: November 27, 2009]

[12] Zuo ZJ, Faghri A. A network thermodynamic analysis of the heat pipe. International Journal of Heat and Mass Transfer. 1998;**41**:1473-1484

[13] Kaya T, Hoang TT. Mathematical Modelling of Loop Heat Pipes; American Institute of Aeronautics and Astronautics (AIAA), Paper No. AIAA 99-04771999. pp. 1-10

[14] Bai L, Lin G, Wen D. Modelling and analysis of start-up of a loop heat pipe. Applied Thermal Engineering. 2000;**30**: 2778-2787

[15] Pauken M, Rodriguez JI. Performance Characterisation and Model Verification of A Loop Heat Pipe; Society of Automotive Engineers (SAE), Paper No. 2000-01-0108; 2000

[16] Hoang TT, Cheung KH, Baldauff RW. Loop Heat Pipe Testing and Analytical Model Verification at the US Naval Research Laboratory, SAE International Paper No. 04ICES-288; 2004

[17] Riehl RR. Comparing the Behaviour of a Loop Heat Pipe with Different Elevations of the Capillary Evaporator, SAE International Paper No. 2004-01-2510; 2004

[18] Zan KJ, Zan CJ, Chen YM, Wu SJ. Analysis of the parameters of the sintered loop heat pipe. Heat Transfer - Asian Research. 2004;**33**:515-526

[19] Riehl RR, Dutra T. Development of an experimental loop heat pipe for application in future space missions. Applied Thermal Engineering. 2005;**25**: 101-112

[20] Vlassov VV, Riehl RR. Modelling of a Loop Heat Pipe for Ground And Space Conditions, SAE International Paper No. 2005-01-2935; 2005

[21] Launay S, Platel V, Dutour S, Joly J-L. Transient modelling of loop

heat pipes for the oscillating behaviour study. Journal of Thermophysics and Heat Transfer. 2007;**21**:487-495

[22] Zhang X et al. Characterization of a solar photovoltaic/loop-heat-pipe heat pump water heating system. Applied Energy. 2013;**102**:1229-1245

[23] Zhang X et al. Dynamic performance of a novel solar photovoltaic/loop-heat- pipe heat pump system. Applied Energy. 2014;**114**: 335-352

[24] He W et al. Theoretical investigation of the thermal performance of a novel solar loop-heat-pipe facade-based heat pump water heating system. Energy and Buildings. 2014;**77**:180-191

[25] Rohsenow W, Hartnet J, Cho Y. Handbook of heat transfer. 3rd ed. New York, USA: McGraw-Hill; 1998

[26] Zhang X et al. Comparative study of a novel liquid-vapour separator incorporated gravitational loop heat pipe against the conventional gravitational straight and loop heat pipes—Part I: Conceptual development and theoretical analyses. Energy Conversion and Management. 2015;**90**: 409-426